Atmospheric
Chemistry
and Physics
Discussions

Open Access

Coherent uncertainty analysis of aerosol measurements from multiple satellite sensors

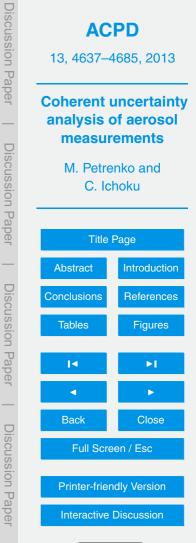M. Petrenko[1,2] and C. Ichoku[2]

[1]Earth System Science Interdisciplinary Center, University of Maryland, College Park, MD, USA
[2]NASA Goddard Space Flight Center, Greenbelt, MD, USA

Correspondence to: M. Petrenko (maksym.petrenko@nasa.gov)

Discussion Paper | Discussion Paper | Discussion Paper | Discussion Paper

ACPD

13, 4637–4685, 2013

Coherent uncertainty analysis of aerosol measurements

M. Petrenko and C. Ichoku

Title Page

Abstract | Introduction

Conclusions | References

Tables | Figures

◄ | ►

◄ | ►

Back | Close

Full Screen / Esc

Printer-friendly Version

Interactive Discussion

Abstract

Aerosol retrievals from multiple spaceborne sensors, including MODIS (on Terra and Aqua), MISR, OMI, POLDER, CALIOP, and SeaWiFS – altogether, a total of 11 different aerosol products – were comparatively analyzed using data collocated with ground-based aerosol observations from the Aerosol Robotic Network (AERONET) stations within the Multi-sensor Aerosol Products Sampling System (MAPSS, http://giovanni.gsfc.nasa.gov/mapss/ and http://giovanni.gsfc.nasa.gov/aerostat/). The analysis was performed by comparing quality-screened satellite aerosol optical depth or thickness (AOD or AOT) retrievals during 2006–2010 to available collocated AERONET measurements globally, regionally, and seasonally, and deriving a number of statistical measures of accuracy. We used a robust statistical approach to detect and remove possible outliers in the collocated data that can bias the results of the analysis. Overall, the proportion of outliers in each of the quality-screened AOD products was within 12 %. Squared correlation coefficient (R^2) values of the satellite AOD retrievals relative to AERONET exceeded 0.6, with R^2 for most of the products exceeding 0.7 over land and 0.8 over ocean. Root mean square error (RMSE) values for most of the AOD products were within 0.15 over land and 0.09 over ocean. We have been able to generate global maps showing regions where the different products present advantages over the others, as well as the relative performance of each product over different landcover types. It was observed that while MODIS, MISR, and SeaWiFS provide accurate retrievals over most of the landcover types, multi-angle capabilities make MISR the only sensor to retrieve reliable AOD over barren and snow/ice surfaces. Likewise, active sensing enables CALIOP to retrieve aerosol properties over bright-surface shrublands more accurately than the other sensors, while POLDER, which is the only one of the sensors capable of measuring polarized aerosols, outperforms other sensors in certain smoke-dominated regions, including broadleaf evergreens in Brazil and South-East Asia.

1   Introduction

Remote sensing of aerosols from space has been a subject of extensive research, with multiple sensors retrieving global aerosol properties on a daily or weekly basis. During the past decade, the retrievals of atmospheric aerosol parameters have been available from a multitude of spaceborne sensors (Lee et al., 2009; Yu et al., 2006). The diverse algorithms used for these retrievals operate on different types of the remotely-sensed signals and rely on different assumptions about the underlying physical phenomena. Significant effort has been made by the various aerosol algorithm teams to progressively refine these assumptions, from algorithm version to version, in order to derive and provide the most accurate products possible. However despite these efforts, measurements of identical aerosol parameters from different sensors, including the most common observable and widely used aerosol optical depth or thickness (AOD or AOT or τ_a) parameter, often disagree with each other due to a variety of reasons including differences in the underlying surface properties at different locations, intrinsic sensor observation characteristics and retrieval approaches (Li et al., 2009). Therefore, it has become necessary to consistently analyze the available aerosol products wherever possible in order to establish the geographical locations where and under what circumstances each of these products provide the greatest accuracy.

The unique attributes of a particular sensor may be advantageous for aerosol retrievals, depending on the parameter(s) being retrieved, especially under favorable atmospheric conditions. However, aerosol retrieval accuracy can also be affected by numerous other factors, including the retrieval algorithm's assumptions and parameterizations, the instrument characteristics (intrinsic design, calibration, and time-dependent degradation), the measurement configurations (solar and view geometry), the atmospheric conditions (cloudiness, aerosol mixing, layer height, and humidity), the surface background (vegetated, bare, snow-covered, inundated, or simply just dark or bright land surface or ocean), and others (Kokhanovsky et al., 2007).

Title Page

Abstract | Introduction

Conclusions | References

Tables | Figures

◄◄ | ►►

◄ | ►

Back | Close

Full Screen / Esc

Printer-friendly Version

Interactive Discussion

Since the accuracy of aerosol retrieval from a sensor may be affected positively or negatively by these factors and conditions in different ways and to varying degrees, a synergetic use of similar aerosol parameters across the sensors is non-trivial and the data synergy research is instead focused on combining orthogonal (i.e. non-conflicting)
5 aerosol measurements. For example, the aerosol layer height information from the Cloud-Aerosol Lidar with Orthogonal Polarization (CALIOP) has been used to enhance aerosol retrievals from other sensors (Oo and Holz, 2011; Torres et al., 2012; Zhang et al., 2011), while the geometry information from the Advanced Along Track Scanning Radiometer (AATSR) was used to initialize the Moderate Resolution Imaging Spectro-
10 radiometer (MODIS) Bi-Directional Reflection Distribution Function (BRDF) in order to derive AATSR AOD (Guo et al., 2009).

To better characterize the differences and uncertainties that exist between the aerosol retrievals from different sensors, several studies compared a limited number of sensors, e.g. AOD retrievals from MODIS were separately compared to retrievals from
15 the MISR Multi-angle Imaging Spectroradiometer (Kahn et al., 2007, 2011; Mishchenko et al., 2010; Zhang and Reid, 2010), the POLDER POLarization and Directionality of the Earth's Reflectances sensor (Gérard et al., 2005), and CALIOP (Kittaka et al., 2011; Redemann et al., 2012). A larger set of sensors was intercompared using a synthetic benchmark (Kokhanovsky et al., 2010), and also based on a detailed analysis
20 of limited geographical regions (Cheng et al., 2012; Yu et al., 2012). In addition, a set of 9 aerosol products was evaluated over ocean and coastal AERONET sites during the period of 1997–2000, highlighting regions of the high retrieval agreement and disagreement (Myhre et al., 2005). However, all the satellite data used in that study had already undergone post-retrieval spatio-temporal aggregation at 1 × 1 degree grid res-
25 olution on a monthly mean basis (so-called Level 3 products) before they were used in the comparisons.

In this work, eleven retrieval-scale (Level 2) aerosol products from multiple spaceborne sensors are intercompared during the recent "golden" period of 2006–2010 (see Fig. 1), when as many as seven major sensors were in operation and measuring

Title Page

Abstract | Introduction

Conclusions | References

Tables | Figures

◄◄ | ►►

◄ | ►

Back | Close

Full Screen / Esc

Printer-friendly Version

Interactive Discussion

aerosols concurrently. Specifically, we focus on aerosol products retrieved over land and ocean from MODIS on Terra and Aqua, MISR on Terra, the Ozone Monitoring Instrument (OMI) on Aura, POLDER on PARASOL, CALIOP on CALIPSO, and the Sea-viewing Wide Field of view Sensor (SeaWiFS) aboard the SeaStar spacecraft. At the time of this study (January 2013), all of the studied sensors are still active, with the exception of SeaWiFS, whose operation ended in December 2010. The analysis is based on the collocation of the satellite data products using the Multi-sensor Aerosol Products Sampling System (MAPSS) framework (Petrenko et al., 2012) that samples these satellite products relatively uniformly over the global AERosol Robotic NETwork (AERONET) of sun-photometers and other important ground-based stations both over land and ocean.

The details of the MAPSS sampling approach are explained in Sect. 2, while the relevant characteristics of the aerosol data products from the different sensors and the corresponding data quality screening techniques are described in Sects. 3 and 4. Section 5 describes a novel statistical approach for detecting and removing possible data outliers that can exist in the collocated data and, as a result, bias the statistical analysis of these data. Section 6 presents the detailed analysis of the compared aerosol products, while Sect. 7 examines the accuracy of these products based on land cover type. Conclusions are presented in Sect. 8.

2 Sampling method

The different aerosol-measuring sensors have different spatial resolutions, of which some have square-shaped footprints while others have rectangular pixel shapes. The nominal ground pixel sizes of the analyzed aerosol products at nadir are summarized in Table 1 and these sizes become progressively larger away from nadir. To ensure a uniform and fair sampling of the aerosol products for cross-evaluation with AERONET and for comparison with one another, we used the framework of Multi-sensor Aerosol Products Sampling System (MAPSS) that was originally developed by Ichoku et al. (Ichoku

Coherent uncertainty analysis of aerosol measurements

M. Petrenko and
C. Ichoku

Title Page

Abstract | Introduction

Conclusions | References

Tables | Figures

◀ | ▶

◀ | ▶

Back | Close

Full Screen / Esc

Printer-friendly Version

Interactive Discussion

M. Petrenko and
C. Ichoku

et al., 2002) for validation and analysis of MODIS aerosol products (Chu et al., 2002; Ichoku et al., 2003, 2005; Levy et al., 2010; Remer, 2002) and later expanded to support aerosol products retrieved by other spaceborne sensors (Petrenko et al., 2012). MAPSS subsets the aerosol products by extracting pixels covering approximately the same area on the ground centered over AERONET sun photometer measurement sites and over certain other point locations that are not addressed in this study.

Assuming an imaginary circle of 55-km diameter whose center coincides with each AERONET station, all spaceborne aerosol product pixels falling within the circle are extracted. An aerosol pixel is regarded as being within the circle if the coordinates of the pixel center fall within 27.5 km from the coordinates of the circle center, where the distance between the coordinates of the two points is determined using the Haversine formula (Sinnott, 1984). Based on the nominal spatial resolution of the sensors in Table 1, the approximate maximum number of pixels within the 55-km diameter sample space at nadir for the different sensors is as follows: MODIS – 25, MISR – 9, OMI – 8, POLDER – 9, CALIOP – 11, and SeaWiFS – 16. The actual number of pixels within the sampling circle decreases for the aerosol retrievals away from the nadir of the satellite scene, and can be further reduced in the presence of clouds or other factors preventing retrieval of aerosol parameters. Based on the extracted sample, statistics of each aerosol parameter retrieved within the sampling areas are calculated and include mean, median, standard deviation, as well as the value of the central pixel over the ground station. In this paper, results are reported based on the analysis of the mean values; although not reported in this paper because of the space considerations, a similar analysis was performed based on the central values and is reported in the digital supplement to this paper. It is appropriate to use the mean values in this paper, so as to maintain the uniform sampling criterion across the different sensors to facilitate a fair intercomparison. Analysis based on central pixel values can provide further details on the effect of difference in sampling aerosol products from individual sensors.

To collocate AERONET data in time and space with the satellite data, AERONET measurements acquired within ±30-min of each satellite sensor overpass are also ex-

tracted and the corresponding statistics are derived. Additionally, for the convenience of aerosol data intercomparison and validation, AERONET AOD are interpolated or (where necessary) extrapolated to the wavelengths of spaceborne sensors in Table 1 based on the established wavelength dependence of AOD (Eck et al., 1999). It is pertinent to note that this interpolation (and particularly) extrapolation process might introduce an additional source of uncertainty when intercomparing the aerosol products, especially for certain stations, where AERONET AOD observations in the range of 440–1200 nm have to be extrapolated by 52 nm to match OMI AOD at 388 nm.

Each AERONET station has a different period of operation and the quantity of available AOD data points is not uniform across all stations; while many stations are still active, certain stations were active in the past and only for a short period of time. The overall availability of the collocated data during the analysis period of 7 June 2006 to 11 December 2010 is shown in Fig. 2, where for the purposes of this study the stations are classified as land-only, ocean-only, or land-and-ocean. This classification is based on analyzing collocated data of separate aerosol retrievals over land and ocean from the MODIS, SeaWiFS, and POLDER sensors and identifying stations that have AOD data points from the land datasets, ocean datasets, or both; note that the MISR, OMI, and CALIOP sensors provide only joint land-and-ocean datasets.

3 Aerosol products

The key properties of the 11 analyzed aerosol products are summarized in Table 1, while the original science data set (SDS) names of the spaceborne aerosol products are outlined in the first column of Table 2, except for the POLDER products that do not have an established SDS product naming convention. The sampled satellite data products are derived directly from the retrieval level aerosol products (Level 2) that represent the highest available spatial resolution for each product/sensor combination and are free of aggregation artifacts that can be present in data at Level 3 (Hyer et al., 2011; Levy et al., 2009; Zhang and Reid, 2010).

Of the 11 sampled products, 3 are combined land-and-ocean products, 6 are land-only products, and 4 are ocean-only products. Furthermore, 6 aerosol products are retrieved from the twin MODIS-Terra and MODIS-Aqua sensors using the same set of 3 algorithms: the ocean algorithm is used for the retrievals over oceans and other large bodies of water, the land Dark Target (DT) algorithm is used over vegetated regions and other dark surfaces (Remer et al., 2005), and the land Deep Blue (DB) algorithm is used for deserts and barren lands (Hsu et al., 2004). Although the results between the two MODIS sensors are expected to be very close, they might still differ due to the different times of scene observation during the day and other factors summarized in (Ichoku et al., 2005; Remer et al., 2008).

The remainder of this section provides a brief description of the analyzed products and highlights some of the unique aerosol properties reported in these products. A more detailed overview can be found in the theoretical and validation works of the respective science teams of the products as cited below, while a general comparative overview of multiple products and retrieval algorithms are in (Kokhanovsky et al., 2007; Lee et al., 2009; Li et al., 2009; Yu et al., 2006).

AERONET (http://aeronet.gsfc.nasa.gov) sun-photometers measure aerosol properties using ground-based observations of solar direct and diffuse irradiances. In this work, the AERONET product used is the aerosol optical depth or thickness (AOD or AOT), which is retrieved from the AERONET direct measurements of solar irradiance. Since AERONET measurements are made from the ground looking up, they present a distinct advantage over spaceborne retrievals in that they are not affected by uncertainties associated with the effects of surface properties as much as satellite measurements are (Dubovik et al., 2002; Holben et al., 1998, 2001). Furthermore, the Level 2.0 AERONET data used in this work are carefully calibrated, cloud screened, and quality assured (Smirnov et al., 2000) and therefore are especially suitable for use as the reference standard against which the satellite aerosol remote-sensing data are evaluated.

The MODIS (http://modis.gsfc.nasa.gov) aerosol product (MOD04 and MYD04) comprises the column aerosol optical thickness and other physical properties of aerosols

Title Page

Abstract | Introduction

Conclusions | References

Tables | Figures

◄ | ►|

◄ | ►

Back | Close

Full Screen / Esc

Printer-friendly Version

Interactive Discussion

retrieved globally over land and ocean (Chu et al., 2002; Hsu et al., 2004; Ichoku et al., 2005; Levy et al., 2010; Remer, 2002; Remer et al., 2005).

The MISR (http://www-misr.jpl.nasa.gov) aerosol product (MIL2ASAE) features aerosol retrievals based on observations from 9 independent camera angles. Multiple viewing angles allow MISR to measure certain aerosol properties that are not available from the other instruments (e.g. aerosol particle size). Furthermore, MISR multiple cameras enable retrievals under conditions that are unfavorable to single-view (e.g. nadir) instruments, such as over bright surfaces or sun glint, where the other instruments are unable to make reliable retrievals in the visible wavelengths (Kahn, 2005; Kahn et al., 2010a; Martonchik et al., 2009).

The OMI (http://www.knmi.nl/omi/research/instrument/index.php) aerosol product (OMAERUV) measures the near-UV (near ultraviolet) aerosol absorption and extinction optical depth, as well as single scattering albedo, among other aerosol properties (Torres et al., 1998, 2007). Moreover, OMI is capable of retrieving absorption optical depth in partially cloudy conditions that usually pose a challenge to other aerosol instruments.

The POLDER onboard PARASOL (http://www.icare.univ-lille1.fr/parasol) aerosol land product (P3L2TLGC) and aerosol ocean product (P3L2TOGC) are derived from measuring spectral, directional, and polarized properties of reflected solar radiation. One of the main features of the POLDER instrument is its utilization of polarization properties of the measured radiation for retrieving anthropogenic aerosol optical depth (Bréon et al., 2002; Buriez et al., 2002; Deuzé et al., 1999, 2001; Herman et al., 1997). It is important to note that the POLDER operational algorithm retrieves AOD at 2 wavelengths (670 and 865 nm) over ocean and only at 1 wavelength (865 nm) over land. Furthermore over land, the POLDER algorithm retrieves only AOD that corresponds to polarized particles, i.e. mainly fine mode particles originating from anthropogenic activities.

The CALIOP (http://www-calipso.larc.nasa.gov) aerosol product (05kmALay) represents daytime and nighttime atmospheric curtain slices portraying the vertical distri-

Coherent uncertainty analysis of aerosol measurements

M. Petrenko and
C. Ichoku

Title Page

Abstract	Introduction
Conclusions	References
Tables	Figures

|◄ | ►|

◄ | ►

Back | Close

Full Screen / Esc

Printer-friendly Version

Interactive Discussion

bution of aerosols and clouds in the atmosphere, including the density and certain properties of individual aerosol layers (Omar et al., 2009; Winker et al., 2007).

The SeaWiFS (http://disc.sci.gsfc.nasa.gov/dust/) aerosol product (SWDB) uses the Deep Blue algorithm to derive aerosol optical thickness and Ångström exponent. The key features of this product are the retrievals of aerosol properties over both bright desert and vegetated surfaces, avoidance of sun glint that improves aerosol retrievals over ocean, and a highly precise calibration of the SeaWiFS sensor (Hsu et al., 2004, 2012).

Since each of the foregoing data sets has a few versions because of the periodic revisions and updates of their retrieval algorithms over time, the data versions that were current at the time of writing this paper (January 2013) were sampled, although the study has been designed in a highly flexible way to enable rapid re-analysis as the new versions become available. The respective data versions used in this paper are: Terra and Aqua MODIS (Collection 051), MISR (Version 002), OMI (Version 003), CALIOP (Version 3-01), POLDER (Versions L and K), SeaWiFS (Version 003), and AERONET AOD (Version 2). Therefore, all of the illustrations and analyses shown in this paper are based on these data versions for the respective aerosol sensors.

4 Data quality screening

While the AERONET Level-2 data are manually inspected to be free of retrieval defects and anomalies (Smirnov et al., 2000), such approach is not feasible for the voluminous spaceborne data. Instead, all Level-2 aerosol products analyzed in this paper assign to AOD pixels one or more quality assurance (QA) flags that indicate a degree of "confidence" of the retrieval algorithms in their results. For MODIS and SeaWiFS, aerosol QA flags are integer numbers ranging from 0 to 3, with 3 representing the highest quality. For MISR and OMI data, the reverse is the case (i.e. 0 is the highest quality). Finally, for POLDER and CALIOP, QA data are a combination of one or more flags, most of which are real numbers ranging between 0 and 1, where 1 indicates the highest quality. By
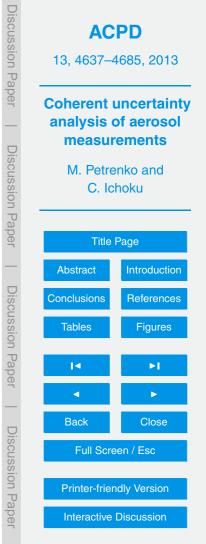
means of these QA flags, certain aerosol retrievals are identified as "bad quality" and are considered to be not trustworthy enough for certain analyses. Therefore, users of these aerosol products have been advised to choose data corresponding to a range of QA values that is most appropriate for their specific needs.

5   To establish similar yet valid QA thresholds for the analyzed products, we consulted science teams of the analyzed products as well as data product validation results reported by these teams and other research groups. Based on this inquiry, we chose the acceptable QA values as described in Table 2. For the majority of the products, the thresholds are set based on selecting a limited subset of the possible QA values.

10 An important exception is the POLDER aerosol products, where the QA flags are expressed as real numbers between 0 ("bad retrieval") and 1 ("excellent retrieval"). Since there are no formal recommendations on the acceptable range of the flag values, we empirically set its threshold to ≥ 0.7, which selects data of a reasonable quality yet discards the minimal number of data pixels (see Fig. 3).

15 The original MAPSS framework was designed to facilitate data analysis experiments based on different values of QA flags. For this, MAPSS extracts QA flags over the sampling area and computes the statistical mode for integer QA flags and mean for real QA flags. These statistical modes of the integer QA flags and means of the real QA flags provide a single number for the quality assessment of each sample set, and

20 can be used to screen the corresponding subset statistics while providing a convenient alternative compared to screening individual pixels, e.g. see (Levy et al., 2010; Remer et al., 2008). However, it was observed that this approach has an unequal impact on the statistical properties of the different aerosol products (Petrenko et al., 2012).

As an example, consider Fig. 4, where the global collocated subset mean AOD values from OMI and Terra MODIS Deep Blue (TMODIS DB) are compared to the cor-

25 responding subset mean AOD values from AERONET. It can be observed that while filtering the mean TMODIS DB AOD values by the mode of QA flags improves the R^2 and RMSE statistics, when compared to computing the mean values based on individually screened TMODIS DB AOD pixels, this filtering significantly changes the

distribution of the collocated data. Specifically, compared to screening individual pixels, QA mode filtering removes 50 % more of the collocated data points and degrades the slope of the fitted regression line as a result of removing certain high-biased points. The opposite behavior can be observed in the collocated OMI AOD and AERONET AOD datasets, where screening by QA mode degrades R^2 of the collocated data when compared to screening individual pixels, although RMSE is still improved and the slope of the fitted regression line remains the same, since both screening approaches produce approximately the same number of the OMI subset data points.

This observation indicates a certain inhomogeneity in the uncertainties that are present in the aerosol products, as in some cases high biases in individual pixels might overwhelm the statistics derived from the sample set. Therefore, to avoid such biases and ensure a fair comparison between the analyzed aerosol products, the rest of this study is based on the QA "pre-filtering" approach, where individual pixels in a spatial sample are screened by their QA values before computing the statistics of this sample. This approach also closely models a typical use of the spaceborne aerosol data, where data users screen each pixel individually and do not consider QA values of its neighboring pixels. The data quantity impact of the described QA screening approach can be observed in Table 3 that provides the sizes of the analyzed datasets before and after the screening. It is noticeable that, depending on the product, the impact is quite different, with the two MODIS ocean AOD datasets and the MISR AOD dataset retaining almost all of their available datasets whereas the two MODIS DT datasets retained only one-fourth of the complete collocated datasets.

It is important however to keep in mind that the QA values reported by the retrieval algorithms are to a large degree subjective to these algorithms and do not always reflect the actual quality of the retrievals. For example, in an absence of a proper aerosol or surface model, an algorithm can in certain cases use a wrong model to retrieve aerosol properties and mistakenly assign this retrieval a "good" QA flag, e.g. (Kahn et al., 2010a; Levy et al., 2010). Furthermore, a retrieval algorithm used might not have enough skill or even the possibility to correctly recognize certain conditions that are

unfavorable for aerosol retrieval, e.g. sub-pixel cloud contamination in OMI retrievals (Torres et al., 1998). In yet another situation, an aerosol scene can be observed in only a portion of the available observation modes of a sensor, e.g. in only a few of the available observation directions in POLDER (Herman et al., 1997), which can lead to more confident yet less reliable results. The opposite case can also be true, where an algorithm correctly retrieves aerosol properties but is not confident about the retrieval. As an example, consider Fig. 5 that explores how QA screening degrades the statistics of OMI AOD and Aqua MODIS Deep Blue AOD datasets when compared to AERONET AOD over Djougou, Benin, as a result of assigning a "bad" QA flag to sufficiently "good" retrievals.

5 Possible data outliers

Under rare circumstances, aerosol retrievals from spaceborne observations can produce aerosol properties that do not reflect the actual physical state of aerosol in the atmosphere. Some of the reasons for such retrievals were discussed in the previous section and might include, but are not limited to, such factors as the lack of a proper aerosol model, incorrect assumptions about boundary conditions, cloud contamination, and several other factors. In Fig. 6, the possible abnormal retrievals can be visually identified by observing points that have a minimal data density and lie abnormally far from the fitted regression lines. Even though an actual fraction of such data points in a complete collocated data set can be relatively minor, the extreme deviations of such points from the overall trend might significantly bias and misrepresent the overall statistics of the data. Therefore, when computing the overall statistics and inter-comparing the aerosol products, such data points should be treated as possible outliers and analyzed separately from the rest of the data.

In order to identify and separate the possible data outliers, we analyzed AOD residuals, i.e. the difference between spaceborne AOD and AERONET AOD observations, using the Modified Z-Score test (Iglewicz and Hoaglin, 1993; National Institute of Stan-

dards and Technology, 2012). This test is designed for testing data for multiple outliers in approximately normal data sets and works by finding data points that differ from the mean value by more than 5 median absolute deviations. Unlike the standard deviation used in the traditional Z-Score test, the median absolute deviation in the Modified Z-Score test is calculated based on the median of the data and is less sensitive to extreme values.

It is pertinent to note that even though AOD data are known to follow the lognormal distribution (O'Neill et al., 2000), the AOD residuals of the analyzed products follow an approximately normal distribution as shown in Figs. 7 and 8, with the exception of the POLDER products that mostly underestimate AOD, because their retrievals focus on anthropogenic aerosols, and thus represent only the negative portion of the distribution. In the figures, it can be seen that the distributions have long tails, strongly indicating a presence of outliers. Furthermore, it can be observed that the slopes of the fitted lines are different from the slope of the 1 : 1 line. This indicates that the standard deviation of the analyzed residuals is different from 1, showing that these data do not follow the standard normal distribution, although this difference does not affect the test since the Modified Z-Score test normalizes residuals by the median absolute deviation of the data.

The overall effect of removing the possible outliers can be observed in the bottom-right sub-plots of Figs. 6–8, as highlighted by the green frames, showing that 926 (6.9 %) outliers are removed from the SeaWiFS Ocean AOD dataset. The total numbers of the removed outliers are provided in Table 3 and do not exceed 12% of the total QA-screened data for any of the datasets when considering the all-season data. The global distribution of the possible data outliers is depicted in Fig. 9 and generally corresponds to the outlier locations reported by the science teams of the aerosol products, e.g. outliers around the coastal areas where the significant subpixel surface variations, shallow waters, sediments, and complex marine/inland aerosol mixtures complicate the retrievals, and also data outliers associated with uncertain retrievals by the MODIS and MISR algorithms in Amazon basin and near the Sahara desert (Kahn et al., 2010a;

Levy et al., 2010), although a more detailed study is needed to determine the specific factors that lead to these outliers and their spatio-temporal distributions, in order to develop appropriate mitigation measures in the retrieval algorithms for each of the products. In the remainder of this paper, the reported results are based on the QA-screened data with the outliers removed.
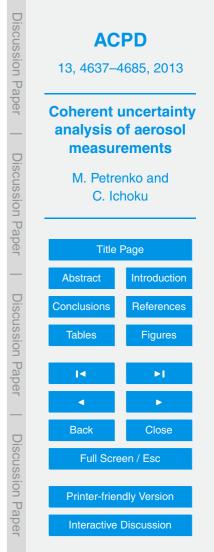
6 Analysis

The overall data distribution for the analyzed spaceborne aerosol products is presented in Fig. 6, whereas the detailed linear regression fit statistics (Fox, 1997) for the products based on the treatment of the possible data outliers and the nominal delimiters of the four boreal seasons, namely, spring (March–May), summer (June–August), autumn (September–November), and winter (December–February), are listed in Table 3. The statistics are presented based on a seasonal timeframes rather than monthly or shorter time periods because there may not be sufficient coincident data for a scatter plot over such shorter time periods, due to the infrequency of satellite aerosol retrieval caused by cloud cover and other issues. Fortunately, many climatic events that are relevant to aerosol emission, transport, and distribution are often roughly aligned with these seasons.

In the presented statistics, the slope value indicates by how much the satellite retrieval for the parameter under consideration is relatively underestimated or overestimated across different magnitudes, depending on whether the slope value is less than or greater than unity. The offset parameter indicates the extent to which the satellite retrieval is biased. The squared linear correlation coefficient (R^2) indicates how consistent the parameter retrieval is across its magnitude range, that is how tightly the points are aligned close to the 1-to-1 line. Finally, the root mean square error (RMSE) indicates the accuracy of the retrievals measured as the average error in the spaceborne retrievals as compared to the ground-based AERONET retrievals.

In Table 3, it can be seen that all MODIS, MISR, and SeaWiFS aerosol products correlate to AERONET observations with $R^2 \geq 0.6$. Furthermore, MISR, SeaWiFS Land, and MODIS Dark Target products have $R^2 \geq 0.7$ and MODIS Ocean products have $R^2 \geq 0.8$. Also, once the possible outliers are removed, the SeaWiFS, MISR, and MODIS Dark Target products reach $R^2 \geq 0.8$, while the MODIS Deep Blue products exceed $R^2 \geq 0.7$. All the best-performing Land products have RMSE values of about 0.15 (measured in the same units as AOD), with the exception of MODIS Deep Blue products that have RMSE of 0.23. Removing possible outliers improves (reduces) the RMSE of all products by 25–50 %, with the exception of OMI for which the improvement is the smallest. This indicates an opportunity for improvement of the aerosol data products by adjusting the retrieval algorithms in the areas with the highest concentrations of the possible outliers.

Figure 10 charts the seasonal dependence of R^2 and RMSE of the spaceborne products based on the data in Table 3. While all of the products demonstrate the high seasonal variations in the statistical parameters, the OMI, CALIOP, POLDER, SeaWiFS, and MODIS Deep Blue are the most sensitive to the seasonal changes in the retrieval conditions, perhaps because of the uncertainties associated with cloud screening (Li et al., 2009), although collocating spaceborne observations with AERONET introduces certain bias towards cloud-free scenes because of the comprehensive AERONET cloud screening procedures (Smirnov et al., 2000). Furthermore, it can be seen that while removing the data outliers greatly reduces the RMSE and removes sensitivity to the seasonal changes in CALIOP, POLDER, and SeaWiFS, the sensitivity remains the same for OMI and MODIS Deep Blue indicating that the retrieval errors reflected by the RMSE of these products likely stem from the regular retrievals rather than the anomalous retrievals.

The accuracy of the spaceborne aerosol products might vary with the location of the retrieval and, depending on the location, some products might be significantly more accurate than others. The spatial dependence of the accuracy of the analyzed products is explored in Figs. 11 and 12, where it can be observed that no single sensor provides

the best retrievals at all sites. Furthermore, as indicated by the lighter shading in Fig. 11 (e.g. Southern Australia) and also in the histogram of R^2 inset in this figure, some sites are not covered by high-correlation (i.e. $R^2 \geq 0.75$) retrievals at all or have no collocated retrievals from the most accurate of the products.
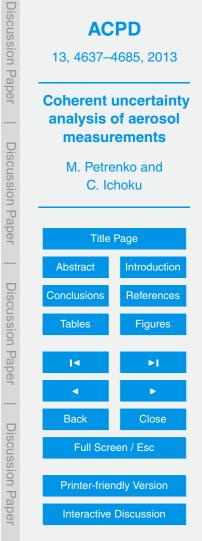
Furthermore, it can be observed that the best-performing aerosol products differ between Figs. 11 and 12 and the products providing the best RMSE are oftentimes those with the lower R^2. Therefore, when choosing an aerosol product for a specific analysis goal and at a specific region, it is necessary to consider a balance between a variety of seasonal, statistical, and spatial factors.

7 Accuracy of aerosol data products based on land cover type

Aerosol properties are derived from satellite observations based on a set of assumptions about the type and the optical properties of the underlying terrestrial surfaces. Therefore, it can be beneficial to compare the accuracy of the considered aerosol data products based on the land cover types of the sites over which the data subsets were extracted. As a reference for land cover types and their spatial extent, we used the global data set that is based on the International Geosphere-Biosphere Programme (IGBP) classification scheme and is available from the suite of MODIS products (Friedl et al., 2002). For each land cover type, we identified coincident AERONET stations and averaged their corresponding statistical results from Sect. 6. Tables 4 and 5 list the results of this aggregation, while Figs. 13 and 14 outline these results on a geographical map.
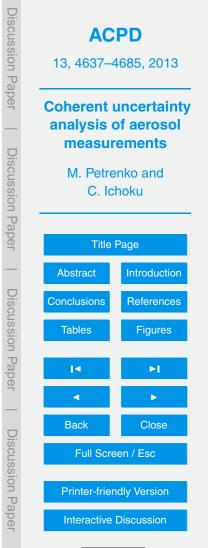
Generally, these aggregated results corroborate the findings of Sect. 6 and the aerosol products from MODIS and MISR sensors produce the most accurate results for the majority of the land cover types, although there are some peculiarities that should be discussed in greater detail in order to better understand the best areas of application of the analyzed aerosol products.

Specifically, IGBP *water* surface locations include 36 AERONET stations out of 154 stations with collocated ocean retrievals identified in Fig. 2. At these 36 locations, MODIS, MISR, and SeaWiFS demonstrate the best results with $R^2 \approx 0.7$. Furthermore, POLDER Ocean data set has a good RMSE = 0.08 (Deuzé et al., 1999) that is compa-

5 rable to the best performing sensors in this region, albeit it has a relatively low squared correlation coefficient value of $R^2 = 0.55$; note that these statistics are different from POLDER Ocean statistics in Fig. 6 that analyzes a more complete set of AERONET stations. It is interesting to note that the correlation between AERONET and Aqua MODIS AOD with $R^2 = 0.8$ is higher than the correlation between AERONET and Terra

10 MODIS AOD with $R^2 = 0.74$. A detailed inspection of the data showed that this difference stems from several AERONET sites with relatively small numbers of collocated data points ($N < 35$) and the average AOD below 0.2. Under such low-AOD conditions, MODIS Ocean algorithm has difficulty in retrieving the precise AOD values and, as a result, is subject to an increased rate of errors (Kleidman et al., 2005; Remer, 2002).

15 *Evergreen broadleaf forest* regions provide conditions that are favorable for retrieving AOD and multiple sensors demonstrate the high correlation with AERONET, including MODIS Dark Target with $R^2 = 0.85$, MISR with $R^2 = 0.89$, SeaWiFS with $R^2 = 0.94$, and POLDER with $R^2 = 0.7$. However, since these regions are also susceptible to complex smoke events (e.g. Ji Parana, Brazil), sometimes combined with dust and pollution

20 events (e.g. Anmyon, S. Korea, Hong Kong, China), most of the sensors demonstrate a rather poor RMSE (Hyer et al., 2011). The important exception is POLDER dataset that has RMSE = 0.07, possibly because POLDER is especially sensitive to small particles produced by biomass burning and anthropogenic pollution sources (Fan et al., 2008), thereby retrieving fairly accurate AOD values at Ji Parana and Lulin, Taiwan. It

25 should be also noted that together with deciduous broadleaf forests and savannas, evergreen broadleaf forest is one of the 3 land cover types where POLDER demonstrates very good results with $R^2 \approx 0.7$, indicating the advantage of polarization measurements for aerosol retrievals over these regions.

Title Page

Abstract | Introduction

Conclusions | References

Tables | Figures

|◄ | ►|

◄ | ►

Back | Close

Full Screen / Esc

Printer-friendly Version

Interactive Discussion

For *mixed forests*, MODIS Dark Target products provide the highest retrieval accuracy with $R^2 = 0.78$ for Terra and 0.82 for Aqua, while MISR data is somewhat less accurate with $R^2 = 0.7$ as a result of underestimating high AODs during summertime biomass burning events (Kahn et al., 2010b), although RMSE = 0.04 of MISR is almost a factor of two better than RMSE = 0.08 of Terra MODIS and RMSE = 0.07 of Aqua MODIS. Sufficiently reliable aerosol data are also retrieved by SeaWiFS with $R^2 = 0.69$ and by POLDER with $R^2 = 0.65$.

For *closed shrubland*, CALIOP with $R^2 = 0.88$ MISR with $R^2 = 0.81$, and MODIS Deep Blue with $R^2 = 0.74$ for Terra and $R^2 = 0.85$ for Aqua produce the best results. Although MODIS Deep Blue shows a better performance than MODIS Dark Target for this land-cover type, the Deep Blue products are retrieved only over a single Lake Argyle AERONET site in northern Australia, whereas Dark Target products are retrieved over 7 sites and have a significantly larger number of data points. Likewise, the best result demonstrated by CALIOP also originates exclusively from the Lake Argyle retrievals. The difference of 0.1 in R^2 between MODIS Terra Deep Blue and MODIS Aqua Deep Blue can be partly explained by the difference in the data availability of these two data sets, as MODIS Terra Deep Blue at the time of this work is availably only through 2007; this effect can be also observed for several other land cover types, where MODIS Aqua Deep Blue tends to have a lower correlation to AERONET and produces results that are closer to the results of SeaWiFS, probably because the latter is also based on the Deep Blue retrieval algorithm (Hsu et al., 2006).

Over *wooded savannas*, both Dark Target and Deep Blue products from MODIS, and SeaWiFS produce very good results with $R^2 \approx 0.85$. MISR with $R^2 = 0.63$ and OMI with $R^2 = 0.66$ produce lower, but still reasonable results. The reduced performance of MISR in this region can be explained by the lack of region-specific aerosol mixtures in its retrieval algorithm, a situation that is expected to be improved in future revisions of the product (Kahn et al., 2009). It should be also noted that this region enables the highest correlation between OMI and AERONET observations, probably as a result of

favorable cloud-free conditions in sub-Saharan Africa (Ahn et al., 2008; Torres et al., 2007).

Open shrublands are very dry and sparsely vegetated regions that are characterized by bright surfaces. Such regions present a great challenge for remote retrieval of aerosol properties (Kahn et al., 2009) and none of the analyzed products exceeded the correlation coefficient of 0.7. Among the best-performing products, CALIOP produced the best results with $R^2 = 0.68$, closely followed by MODIS Dark Target with $R^2 = 0.67$ for Terra and $R^2 = 0.62$ for Aqua, MISR with $R^2 = 0.64$, and MODIS Deep Blue with $R^2 = 0.52$ for Terra and $R^2 = 0.65$ for Aqua. It should be noted that open shrublands and closed shrublands are the two areas where CALIOP outperforms other sensors, possibly indicating the advantage of active aerosol sensing over these bright-surface regions.

Similar to open shrublands, *grasslands* were challenging to all of the sensors, where Terra MODIS Deep Blue with $R^2 = 0.73$ and MISR with $R^2 = 0.7$ demonstrated the best results. Even more challenging were *snow and ice* and also *barren or sparsely vegetated* areas, where MISR was the only highly accurate aerosol product with $R^2 = 0.83$ for snow/ice and $R^2 = 0.78$ for barren lands, thanks to its multi-angle measurement capabilities that allow retrieving aerosol properties over bright surfaces and enable the advanced cloud and ice detection capabilities (Kahn et al., 2009).

8 Conclusions

In this paper, we analyzed and intercompared 11 spaceborne aerosol products from MODIS, MISR, OMI, SeaWiFS, POLDER, and CALIOP sensors, which were sampled fairly uniformly based on the MAPSS framework that was used to collocate these spaceborne observations with ground-based AERONET observations during the period of 7 June 2006 and 11 December 2010, when all the sensors were operational. Based on this analysis, for each of the AERONET stations, we identified products providing the best correlation coefficient (R^2) and root mean square error (RMSE). It was

found that no single product provides the best retrieval over all sites, and certain sites are not covered by accurate retrievals at all. Furthermore, it was observed that a product providing the best R^2 at a certain location does not always provide the best RMSE at the same location. Therefore, to facilitate the multivariate analysis that is necessary when choosing the most suitable spaceborne aerosol product at a specific region, we plan to develop an interactive tool that would allow exploration of the multi-sensor collocated data on an interactive map.

Further, a statistical approach based on the statistical Modified Z-Score test has been used to automatically identify possible data outliers in collocated data sets. The reported analysis shows that even though such atypical data points constitute a relatively minor portion (3 %–12 %) of the analyzed data sets, they can significantly bias the results of the statistical analysis. For this reason, it is suggested that such data points be set aside when analyzing collocated data sets and inspected separately.

Finally, we assessed the accuracy of the spaceborne aerosol products based on IGBP land cover classification scheme. This analysis identified sensors that retrieve the most accurate aerosol properties over each of the defined land cover types and highlighted the differences that exists between the sensors, providing an advantage or disadvantage in retrieving AOD over the areas of a particular land cover type. Notably, some of the land cover types, including open shrublands and grasslands, had only moderately accurate retrievals, indicating the need for improved spaceborne aerosol remote sensing instrumentation/approaches and/or retrieval algorithms.

Supplementary material related to this article is available online at:
http://www.atmos-chem-phys-discuss.net/13/4637/2013/
acpd-13-4637-2013-supplement.pdf.

References

Ahn, C., Torres, O., and Bhartia, P. K.: Comparison of ozone monitoring instrument UV aerosol products with aqua/moderate resolution imaging spectroradiometer and multiangle imaging spectroradiometer observations in 2006, J. Geophys. Res., 113, D16S27, doi:10.1029/2007JD008832, 2008.

Bréon, F. M. M., Buriez, J. C. C., Couvert, P., Deschamps, P. Y. Y., Deuzé, J. L. L., Herman, M., Goloub, P., Leroy, M., Lifermann, A., Moulin, C., Parol, F., Sèze, G., Tanré, D., Vanbauce, C., and Vesperini, M.: Scientific results from the Polarization and Directionality of

Title Page

Abstract | Introduction

Conclusions | References

Tables | Figures

|◀ | ▶|

◀ | ▶

Back | Close

Full Screen / Esc

Printer-friendly Version

Interactive Discussion

the Earth's Reflectances (POLDER), Adv. Space Res., 30, 2383–2386, doi:10.1016/S0273-1177(02)80282-4, 2002.

Cheng, T., Chen, H., Gu, X., Yu, T., Guo, J., and Guo, H.: The inter-comparison of MODIS, MISR and GOCART aerosol products against AERONET data over China, J. Quant. Spectrosc. Ra., doi:10.1016/j.jqsrt.2012.06.016, 2012.

Chu, D. A., Kaufman, Y. J., Ichoku, C., Remer, L. A., Tanré, D., and Holben, B. N.: Validation of MODIS aerosol optical depth retrieval over land, Geophys. Res. Lett., 29, 8007, doi:10.1029/2001GL013205, 2002.

Deuzé, J. L., Herman, M., Goloub, P., Tanré, D., and Marchand, A.: Characterization of aerosols over ocean from POLDER/ADEOS-1, Geophys. Res. Lett., 26, 1421–1424, doi:10.1029/1999GL900168, 1999.

Deuzé, J. L., Bréon, F. M., Devaux, C., Goloub, P., Herman, M., Lafrance, B., Maignan, F., Marchand, A., Nadal, F., Perry, G., and Tanré, D.: Remote sensing of aerosols over land surfaces from POLDER-ADEOS-1 polarized measurements, J. Geophys. Res., 106, 4913–4926, doi:10.1029/2000JD900364, 2001.

Dubovik, O., Holben, B., Eck, T. F., Smirnov, A., Kaufman, Y. J., King, M. D., Tanré, D., and Slutsker, I.: Variability of absorption and optical properties of key aerosol types observed in worldwide locations, J. Atmos. Sci., 59, 590–608, doi:10.1175/1520-0469(2002)059<0590:VOAAOP>2.0.CO;2, 2002.

Eck, T. F., Holben, B. N., Reid, J. S., Dubovik, O., Smirnov, A., O'Neill, N. T., Slutsker, I., and Kinne, S.: Wavelength dependence of the optical depth of biomass burning, urban, and desert dust aerosols, J. Geophys. Res., 104, 31333–31349, doi:10.1029/1999JD900923, 1999.

Fan, X., Goloub, P., Deuzé, J.-L., Chen, H., Zhang, W., Tanré, D., and Li, Z.: Evaluation of PARASOL aerosol retrieval over North East Asia, Remote Sens. Environ., 112, 697–707, doi:10.1016/j.rse.2007.06.010, 2008.

Fox, J.: Applied Regression Analysis, Linear Models, and Related Methods, Sage Publications, Inc., Newbury Park, CA, USA, 1997.

Friedl, M., McIver, D., Hodges, J. C., Zhang, X., Muchoney, D., Strahler, A., Woodcock, C., Gopal, S., Schneider, A., Cooper, A., Baccini, A., Gao, F., and Schaaf, C.: Global land cover mapping from MODIS: algorithms and early results, Remote Sens. Environ., 83, 287–302, doi:10.1016/S0034-4257(02)00078-0, 2002.

Title Page

Abstract	Introduction
Conclusions	References
Tables	Figures

◄◄ | ►►

◄ | ►

Back | Close

Full Screen / Esc

Printer-friendly Version

Interactive Discussion

Gérard, B., Deuzé, J.-L., Herman, M., Kaufman, Y. J., Lallart, P., Oudard, C., Remer, L. A., Roger, B., Six, B., and Tanré, D.: Comparisons between POLDER 2 and MODIS/Terra aerosol retrievals over ocean, J. Geophys. Res., 110, 1–15, doi:10.1029/2005JD006218, 2005.

Guo, J., Xue, Y., Cao, C., Zhang, H., Guang, J., Zhang, X., and Li, X.: A synergic algorithm for retrieval of aerosol optical depth over land, Adv. Atmos. Sci., 26, 973–983, doi:10.1007/s00376-009-7218-4, 2009.

Herman, M., Deuzé, J. L., Devaux, C., Goloub, P., Bréon, F. M., and Tanré, D.: Remote sensing of aerosols over land surfaces including polarization measurements and application to POLDER measurements, J. Geophys. Res., 102, 17039–17049, doi:10.1029/96JD02109, 1997.

Holben, B. N., Eck, T. F., Slutsker, I., Tanré, D., Buis, J. P., Setzer, A., Vermote, E., Reagan, J. A., Kaufman, Y. J., Nakajima, T., Lavenu, F., Jankowiak, I., and Smirnov, A.: AERONET – a federated instrument network and data archive for aerosol characterization, Remote Sens. Environ., 66, 1–16, doi:10.1016/S0034-4257(98)00031-5, 1998.

Holben, B. N., Tanré, D., Smirnov, A., Eck, T. F., Slutsker, I., Abuhassan, N., Newcomb, W. W., Schafer, J. S., Chatenet, B., Lavenu, F., Kaufman, Y. J., Castle, J. Vande, Setzer, A., Markham, B., Clark, D., Frouin, R., Halthore, R., Karneli, A., O'Neill, N. T., Pietras, C., Pinker, R. T., Voss, K., and Zibordi, G.: An emerging ground-based aerosol climatology: Aerosol optical depth from AERONET, J. Geophys. Res., 106, 12067–12097, doi:10.1029/2001JD900014, 2001.

Hsu, N. C., Tsay, S.-C., King, M. D., and Herman, J. R.: Aerosol properties over bright-reflecting source regions, IEEE T. Geosci. Remote Sens., 42, 557–569, doi:10.1109/TGRS.2004.824067, 2004.

Hsu, N. C., Gautam, R., Sayer, a. M., Bettenhausen, C., Li, C., Jeong, M. J., Tsay, S.-C., and Holben, B. N.: Global and regional trends of aerosol optical depth over land and ocean using SeaWiFS measurements from 1997 to 2010, Atmos. Chem. Phys. Discuss., 12, 8465–8501, doi:10.5194/acpd-12-8465-2012, 2012.

Hyer, E. J., Reid, J. S., and Zhang, J.: An over-land aerosol optical depth data set for data assimilation by filtering, correction, and aggregation of MODIS Collection 5 optical depth retrievals, Atmos Meas. Tech., 4, 379–408, doi:10.5194/amt-4-379-2011, 2011.

Ichoku, C., Chu, D. A., Mattoo, S., Kaufman, Y. J., Remer, L. A., Tanré, D., Slutsker, I., and Holben, B. N.: A spatio-temporal approach for global validation and analysis of MODIS aerosol products, Geophys. Res. Lett., 29, 1–4, doi:10.1029/2001GL013206, 2002.

Ichoku, C., Remer, L. A., Kaufman, Y. J., Levy, R., Chu, D. A., Tanré, D., and Holben, B. N.: MODIS observation of aerosols and estimation of aerosol radiative forcing over southern Africa during SAFARI 2000, J. Geophys. Res., 108, 8499, doi:10.1029/2002JD002366, 2003.

Ichoku, C., Remer, L. A., and Eck, T. F.: Quantitative evaluation and intercomparison of morning and afternoon Moderate Resolution Imaging Spectroradiometer (MODIS) aerosol measurements from Terra and Aqua, J. Geophys. Res., 110, doi:10.1029/2004JD004987, 2005.

Iglewicz, B. and Hoaglin, D. C.: How to Detect and Handle Outliers, American Society for Quality Control, Milwaukee, WI, 1993.

Kahn, R. A.: Multiangle Imaging Spectroradiometer (MISR) global aerosol optical depth validation based on 2 years of coincident Aerosol Robotic Network (AERONET) observations, J. Geophys. Res., 110, 1–16, doi:10.1029/2004JD004706, 2005.

Kahn, R. A., Garay, M. J., Nelson, D. L., Yau, K. K., Bull, M. A., Gaitley, B. J., Martonchik, J. V., and Levy, R. C.: Satellite-derived aerosol optical depth over dark water from MISR and MODIS: Comparisons with AERONET and implications for climatological studies, J. Geophys. Res., 112, D18205, doi:10.1029/2006JD008175, 2007.

Kahn, R. A., Nelson, D. L., Garay, M. J., Levy, R. C., Bull, M. A., Diner, D. J., Martonchik, J. V., Paradise, S. R., Hansen, E. G., and Remer, L. A.: MISR Aerosol Product Attributes and Statistical Comparisons With MODIS, IEEE Trans. Geosci. Remote Sens., 47, 4095–4114, doi:10.1109/TGRS.2009.2023115, 2009.

Kahn, R. A., Gaitley, B. J., Garay, M. J., Diner, D. J., Eck, T. F., Smirnov, A., and Holben, B. N.: Multiangle Imaging SpectroRadiometer global aerosol product assessment by comparison with the Aerosol Robotic Network, J. Geophys. Res., 115, doi:10.1029/2010JD014601, 2010a.

Kahn, R. A., Gaitley, B. J., Garay, M. J., Diner, D. J., Eck, T. F., Smirnov, A., and Holben, B. N.: Multiangle Imaging SpectroRadiometer global aerosol product assessment by comparison with the Aerosol Robotic Network, J. Geophys. Res., 115, doi:10.1029/2010JD014601, 2010b.

Kahn, R. A., Garay, M. J., Nelson, D. L., Levy, R. C., Bull, M. A., Diner, D. J., Martonchik, J. V., Hansen, E. G., Remer, L. A., and Tanré, D.: Response to "Toward unified satellite climatology

Title Page

Abstract | Introduction

Conclusions | References

Tables | Figures

|◀ | ▶|

◀ | ▶

Back | Close

Full Screen / Esc

Printer-friendly Version

Interactive Discussion

of aerosol properties. 3. MODIS versus MISR versus AERONET", J. Quant. Spectrosc. Ra., 112, 901–909, doi:10.1016/j.jqsrt.2010.11.001, 2011.

Kittaka, C., Winker, D. M., Vaughan, M. A., Omar, A., and Remer, L. A.: Intercomparison of column aerosol optical depths from CALIPSO and MODIS-Aqua, Atmos. Meas. Tech., 4, 131–141, doi:10.5194/amt-4-131-2011, 2011.

Kleidman, R. G., O'Neill, N. T., Remer, L. a., Kaufman, Y. J., Eck, T. F., Tanré, D., Dubovik, O., and Holben, B. N.: Comparison of Moderate Resolution Imaging Spectroradiometer (MODIS) and Aerosol Robotic Network (AERONET) remote-sensing retrievals of aerosol fine mode fraction over ocean, J. Geophys. Res., 110, D22205, doi:10.1029/2005JD005760, 2005.

Kokhanovsky, A. A., Breon, F.-M., Cacciari, A., Carboni, E., Diner, D., Di Nicolantonio, W., Grainger, R. G., Grey, W. M. F., Höller, R., Lee, K.-H., Li, Z., North, P. R. J., Sayer, A. M., Thomas, G. E., and Von Hoyningen-Huene, W.: Aerosol remote sensing over land: a comparison of satellite retrievals using different algorithms and instruments, Atmos. Res., 85, 372–394, doi:10.1016/j.atmosres.2007.02.008, 2007.

Kokhanovsky, A. A., Deuzé, J. L., Diner, D. J., Dubovik, O., Ducos, F., Emde, C., Garay, M. J., Grainger, R. G., Heckel, A., Herman, M., Katsev, I. L., Keller, J., Levy, R., North, P. R. J., Prikhach, A. S., Rozanov, V. V., Sayer, A. M., Ota, Y., Tanré, D., Thomas, G. E., and Zege, E. P.: The inter-comparison of major satellite aerosol retrieval algorithms using simulated intensity and polarization characteristics of reflected light, Atmos. Meas. Tech., 3, 909–932, doi:10.5194/amt-3-909-2010, 2010.

Lee, K., Li, Z., and Kim, Y.: Atmospheric aerosol monitoring from satellite observations: A history of three decades, in: Proceedings of Atmospheric and Biological Environmental Monitoring, edited by: Kim, Y. J., Platt, U., Gu, M. B., and Iwahashi, H., Berlin, Germany, Springer, doi:10.1007/978-1-4020-9674-7, 13–38, 2009.

Levy, R. C., Leptoukh, G. G., Kahn, R., Zubko, V., Gopalan, A., and Remer, L. A.: A critical look at deriving monthly aerosol optical depth from satellite data, IEEE Trans. Geosci. Remote Sens., 47, 2942–2956, doi:10.1109/TGRS.2009.2013842, 2009.

Levy, R. C., Remer, L. A., Kleidman, R. G., Mattoo, S., Ichoku, C., Kahn, R., and Eck, T. F.: Global evaluation of the Collection 5 MODIS dark-target aerosol products over land, Atmos. Chem. Phys., 10, 10399–10420, doi:10.5194/acp-10-10399-2010, 2010.

Li, Z., Zhao, X., Kahn, R., Mishchenko, M., Remer, L., Lee, K.-H., Wang, M., Laszlo, I., Nakajima, T., and Maring, H.: Uncertainties in satellite remote sensing of aerosols and impact on

monitoring its long-term trend: a review and perspective, Ann. Geophys., 27, 2755–2770, doi:10.5194/angeo-27-2755-2009, 2009.

Martonchik, J. V., Kahn, R. A., and Diner, D. J.: Retrieval of aerosol properties over land using MISR observations, in: Proceedings of Satellite Aerosol Remote Sensing over Land, edited by: Kokhanovsky, A. A. and Leeuw, G., Berlin, Germany, Springer, doi:10.1007/978-3-540-69397-0_9, 267–293, 2009.

Mishchenko, M. I., Liu, L., Geogdzhayev, I. V., Travis, L. D., Cairns, B., and Lacis, A. A.: Toward unified satellite climatology of aerosol properties., J. Quant. Spectrosc. Ra., 111, 540–552, doi:10.1016/j.jqsrt.2009.11.003, 2010.

Myhre, G., Stordal, F., Johnsrud, M., Diner, D. J., Geogdzhayev, I. V., Haywood, J. M., Holben, B. N., Holzer-Popp, T., Ignatov, A., Kahn, R. A., Kaufman, Y. J., Loeb, N., Martonchik, J. V., Mishchenko, M. I., Nalli, N. R., Remer, L. A., Schroedter-Homscheidt, M., Tanré, D., Torres, O., and Wang, M.: Intercomparison of satellite retrieved aerosol optical depth over ocean during the period September 1997 to December 2000, Atmos. Chem. Phys., 5, 1697–1719, doi:10.5194/acp-5-1697-2005, 2005.

National Institute of Standards and Technology: Engineering Statistics Handbook, http://itl.nist.gov/div898/handbook/ (last access: 8 February 2013), 2012.

Omar, A. H., Winker, D. M., Vaughan, M. A., Hu, Y., Trepte, C. R., Ferrare, R. A., Lee, K.-P., Hostetler, C. A., Kittaka, C., Rogers, R. R., Kuehn, R. E., and Liu, Z.: The CALIPSO automated aerosol classification and lidar ratio selection algorithm, J. Atmos. Ocean. Technol., 26, 1994–2014, doi:10.1175/2009JTECHA1231.1, 2009.

Oo, M. and Holz, R.: Improving the CALIOP aerosol optical depth using combined MODIS-CALIOP observations and CALIOP integrated attenuated total color ratio, J. Geophys. Res., 116, D14201, doi:10.1029/2010JD014894, 2011.

O'Neill, N. T., Ignatov, A., Holben, B. N., and Eck, T. F.: The lognormal distribution as a reference for reporting aerosol optical depth statistics; Empirical tests using multi-year, multi-site AERONET sunphotometer data, Geophys. Res. Lett., 27, 3333–3336, doi:10.1029/2000GL011581, 2000.

Petrenko, M., Ichoku, C., and Leptoukh, G.: Multi-sensor Aerosol Products Sampling System (MAPSS), Atmos. Meas. Tech., 5, 913–926, doi:10.5194/amt-5-913-2012, 2012.

Redemann, J., Vaughan, M. A., Zhang, Q., Shinozuka, Y., Russell, P. B., Livingston, J. M., Kacenelenbogen, M., and Remer, L. A.: The comparison of MODIS-Aqua (C5) and CALIOP

Title Page

Abstract | Introduction

Conclusions | References

Tables | Figures

◀◀ | ▶▶

◀ | ▶

Back | Close

Full Screen / Esc

Printer-friendly Version

Interactive Discussion

(V2 & V3) aerosol optical depth, Atmos. Chem. Phys., 12, 3025–3043, doi:10.5194/acp-12-3025-2012, 2012.

Remer, L. A.: Validation of MODIS aerosol retrieval over ocean, Geophys. Res. Lett., 29, 8008, doi:10.1029/2001GL013204, 2002.

Remer, L. A., Kaufman, Y. J., Tanré, D., Mattoo, S., Chu, D. A., Martins, J. V., Li, R.-R., Ichoku, C., Levy, R. C., Kleidman, R. G., Eck, T. F., Vermote, E., and Holben, B. N.: The MODIS aerosol algorithm, products, and validation, J. Atmos. Sci., 62, 947–973, doi:10.1175/JAS3385.1, 2005.

Remer, L. A., Kleidman, R. G., Levy, R. C., Kaufman, Y. J., Tanré, D., Mattoo, S., Martins, J. V., Ichoku, C., Koren, I., Yu, H., and Holben, B. N.: Global aerosol climatology from the MODIS satellite sensors, J. Geophys. Res., 113, 1–18, doi:10.1029/2007JD009661, 2008.

Sinnott, R. W.: Virtues of the Haversine, Sky Telescope, 68, 159, 1984.

Smirnov, A., Holben, B. N., Eck, T. F., Dubovik, O., and Slutsker, I.: Cloud-Screening and Quality Control Algorithms for the AERONET Database, Remote Sens. Environ., 73, 337–349, doi:10.1016/S0034-4257(00)00109-7, 2000.

Torres, O., Bhartia, P. K., Herman, J. R., Ahmad, Z., and Gleason, J.: Derivation of aerosol properties from satellite measurements, J. Geophys. Res., 103, 17099–17110, doi:10.1029/98JD00900, 1998.

Torres, O., Tanskanen, A., Veihelmann, B., Ahn, C., Braak, R., Bhartia, P. K., Veefkind, P., and Levelt, P.: Aerosols and surface UV products from Ozone Monitoring Instrument observations: an overview, J. Geophys. Res., 112, 1–14, doi:10.1029/2007JD008809, 2007.

Torres, O., Jethva, H., and Bhartia, P. K.: Retrieval of Aerosol Optical Depth above Clouds from OMI Observations: Sensitivity Analysis and Case Studies, J. Atmos. Sci., 69, 1037–1053, doi:10.1175/JAS-D-11-0130.1, 2012.

Winker, D. M., Hunt, W. H., and McGill, M. J.: Initial performance assessment of CALIOP, Geophys. Res. Lett., 34, 1–5, doi:10.1029/2007GL030135, 2007.

Yu, H., Kaufman, Y. J., Chin, M., Feingold, G., Remer, L. a., Anderson, T. L., Balkanski, Y., Bellouin, N., Boucher, O., Christopher, S., DeCola, P., Kahn, R., Koch, D., Loeb, N., Reddy, M. S., Schulz, M., Takemura, T., and Zhou, M.: A review of measurement-based assessments of the aerosol direct radiative effect and forcing, Atmos. Chem. Phys., 6, 613–666, doi:10.5194/acp-6-613-2006, 2006.

Yu, H., Zhang, Y., Chin, M., Liu, Z., Omar, A., Remer, L. A., Yang, Y., Yuan, T., and Zhang, J.: An integrated analysis of aerosol above clouds from A-Train multi-sensor measurements, Remote Sens. Environ., 121, 125–131, doi:10.1016/j.rse.2012.01.011, 2012.

Zhang, J. and Reid, J. S.: A decadal regional and global trend analysis of the aerosol optical depth using a data-assimilation grade over-water MODIS and Level 2 MISR aerosol products, Atmos. Chem. Phys., 10, 18879–18917, doi:10.5194/acp-10-10949-2010, 2010.

Zhang, J., Campbell, J. R., Reid, J. S., Westphal, D. L., Baker, N. L., Campbell, W. F., and Hyer, E. J.: Evaluating the impact of assimilating CALIOP-derived aerosol extinction profiles on a global mass transport model, Geophys. Res. Lett., 38, 1–6, doi:10.1029/2011GL047737, 2011.
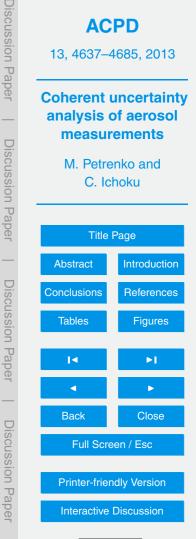
Coherent uncertainty analysis of aerosol measurements

M. Petrenko and
C. Ichoku

Title Page

Abstract	Introduction
Conclusions	References
Tables	Figures

|◄ | ►|

◄ | ►

Back | Close

Full Screen / Esc

Printer-friendly Version

Interactive Discussion

Table 1. Ground-based and spaceborne atmospheric aerosol products analyzed in the study. In the product designation titles, "O" at the end of the title of a product signifies ocean retrievals, "L" – land retrievals, "DT" – land retrievals using the MODIS Dark Target algorithm, and "DB" – land retrievals using the MODIS Deep Blue algorithm. The AERONET AOD retrievals were interpolated or extrapolated to the studied wavelengths of the spaceborne sensors. The indicated local equatorial crossing times are based on the original orbital designs, and can change during the lifetimes of the satellites. SeaWiFS mission has ended in December 2010.

Sensor	Platform	Product	Designation in the study	Study wavelength	Spatial resolution (km × km)	Equator crossing time	Launch date
AERONET	N/A	AOT	AERONET	Varies	N/A	N/A	Varies
MODIS	Terra	MOD04	TMODIS DT TMODIS DB TMODIS O	550 nm	10 × 10	10:30 a.m.	Jan 2000 Jul 2002
	Aqua	MYD04	AMODIS DT AMODIS DB AMODIS O			01:30 p.m.	
MISR	Terra	MIL2ASAE	MISR	558 nm	17.6 × 17.6	10:30 a.m.	Jan 2000
OMI	Aura	OMAERUV	OMI	388 nm	13.7 × 23.7	01:38 p.m.	Oct 2004
POLDER	PARASOL	P3L2TLGC P3L2TOGC	POLDER3 L POLDER3 O	865 nm 670 nm	19 × 19	01:30 p.m.	Mar 2005
CALIOP	CALIPSO	05kmALay	CALIOP	532 nm	5 × 0.1	01:32 p.m.	Jun 2006
SeaWiFS	SeaStar	SWDB	SeaWiFS L SeaWiFS O	550 nm	13.5 × 13.5	12:00 p.m.	Jan 1998

Title Page

Abstract | Introduction

Conclusions | References

Tables | Figures

◄◄ | ►►

◄ | ►

Back | Close

Full Screen / Esc

Printer-friendly Version

Interactive Discussion

Table 2. Studied aerosol data sets, the matching data quality (QA) data sets, and the corresponding QA data screening criteria. Where provided, numbers in parenthesis in the middle column indicate the base-1 layer index, base-0 bit number, and number of bits extracted from this QA data set. For MODIS, MISR, OMI, and SeaWiFS the QA values are integer numbers between 0 and 3, where for MODIS and SeaWiFS larger numbers indicate a better retrieval quality and for OMI and MISR the opposite is true. For POLDER, QA is real number between 0 (worst) and 1 (best). For CALIOP, the QA condition is applied to all layers found in a column; the whole column is rejected if at least one layer fails the test. The listed extinction QC values indicate retrievals that are unconstrained, constrained, have a reduced lidar ratio, or detected an opaque aerosol layer. CAD score and layer type and subtype flags indicate retrievals that classified a layer with a high confidence as containing aerosol and were able to determine the aerosol type. IAB condition is set to prevent the retrieval anomaly of overcorrecting the attenuation of overlaying layers (Kittaka et al., 2011).

AOD data set	QA data set (layer/starting bit/number of bits)	QA condition
MODIS		
Corrected_Optical_Depth_Land	Quality_Assurance_Land (1/1/3)	QA = 3
Deep_Blue_Aerosol_Optical _Depth_550_Land	Quality_Assurance_Land (5/1/2)	QA = 3
Effective_Optical_Depth _Average_Ocean	Quality_Assurance_Ocean (1/5/3)	QA = [1, 2, 3]
MISR		
RegBestEstimateSpectralOptDepth	RegBestEstimateQA	QA = [0, 1]
OMI		
FinalAerosolOpticalDepth	FinalAlgorithmFlags	QA = 0
SeaWiFS		
aerosol_optical_thickness_550_land	aerosol_optical_thickness _confidence_flag_land	QA = 3
aerosol_optical_thickness_550_ocean	aerosol_optical_thickness _confidence_flag_ocean	QA = [2, 3]
CALIOP		
Column_Optical_Depth_Aerosols_532	ExtinctionQC_[532 and 1064]	QA = [0, 1, 2, 16, 18]
	CAD_Score	$-100 \leq$ CAD < -20
	Feature_Classification_Flags (1/0/3)	Layer type = 3
	Feature_Classification_Flags (1/9/3)	Layer subtype > 0
	Integrated_Attenuated _Backscatter_[532 and 1064]	IAB <= 0.01
POLDER		
Aerosol optical thickness at 865 nm corresponding to the polarized particles	Quality index for the inversion	QA $\geq$ 0.7
Aerosol Optical Thickness at 670 nm	Quality index for the inversion	QA $\geq$ 0.7

Title Page

Abstract | Introduction

Conclusions | References

Tables | Figures

◀ | ▶

◀ | ▶

Back | Close

Full Screen / Esc

Printer-friendly Version

Interactive Discussion

Table 3. Statistics of the studied aerosol data sets based on all AERONET stations during the period of 7 June 2006 and 11 December 2010. "N_{tot}" indicates the total number of the collocated Spaceborne AOD – AERONET AOD data points, while "N_{filt}" indicates the number of data points after filtering (screening) the spaceborne data by QA as described in Sect. 4 and Table 2. "N_{out}" is the total number of the possible data outliers determined as explained in Sect. 5. The last 8 columns present the statistics on the collocated data based on regression fits also plotted in Fig. 6.

Dataset	N_{filt}	$N_{filt}/$ N_{tot} (%)	N_{out}	$N_{filt}/$ N_{out} (%)	Complete data				Outliers removed			
					R^2	RMSE	Slope	Intercept	R^2	RMSE	Slope	Intercept
All seasons												
TMODIS DT	56 803	72.9	1711	3.0	0.79	0.11	0.96	0.01	0.83	0.08	0.95	0.00
TMODIS DB	4431	32.2	274	6.2	0.63	0.23	0.87	0.06	0.73	0.14	0.88	0.04
TMODIS O	17 243	99.7	703	4.1	0.82	0.08	1.02	0.03	0.88	0.05	0.96	0.03
AMODIS DT	48 555	68.6	1880	3.9	0.78	0.11	0.97	0.01	0.83	0.08	0.97	0.01
AMODIS DB	13 544	33.9	973	7.2	0.63	0.23	0.88	0.06	0.77	0.14	0.9	0.03
AMODIS O	17 790	99.6	844	4.7	0.8	0.08	0.94	0.03	0.87	0.05	0.93	0.03
MISR	16 561	99.9	959	5.8	0.73	0.13	0.61	0.07	0.84	0.06	0.85	0.03
OMI	52 498	95.6	2009	3.8	0.4	0.25	0.72	0.17	0.51	0.19	0.76	0.14
CALIOP	1885	92.4	158	8.4	0.34	0.23	0.49	0.07	0.66	0.11	0.78	0.00
POLDER3 L	31 874	86.4	3837	12	0.27	0.21	0.17	0.02	0.57	0.08	0.5	−0.01
POLDER3 O	5400	59.8	518	9.6	0.39	0.16	0.25	0.03	0.6	0.07	0.57	0.00
SeaWiFS L	18 305	43.3	1038	5.7	0.75	0.13	0.74	0.04	0.82	0.08	0.88	0.01
SeaWiFS O	13 333	82.6	926	6.9	0.65	0.12	0.99	0.03	0.81	0.06	0.92	0.02
Fall												
TMODIS DT	15 586	72.2	466	3.0	0.83	0.11	1.02	−0.01	0.86	0.07	0.94	0.00
TMODIS DB	1422	29.6	60	4.2	0.48	0.19	0.91	0.03	0.58	0.13	0.86	0.03
TMODIS O	5120	99.6	184	3.6	0.79	0.07	0.91	0.03	0.86	0.05	0.95	0.03
AMODIS DT	12 659	65.9	494	3.9	0.82	0.1	1.03	−0.01	0.86	0.07	0.96	0.00
AMODIS DB	3927	32.4	258	6.6	0.59	0.2	0.97	0.02	0.74	0.12	0.9	0.01
AMODIS O	5135	99.6	271	5.3	0.74	0.07	0.79	0.04	0.86	0.04	0.9	0.02
MISR	4466	99.8	286	6.4	0.7	0.14	0.54	0.07	0.84	0.05	0.83	0.03
OMI	13 909	94.1	661	4.8	0.33	0.22	0.65	0.15	0.48	0.16	0.72	0.11
CALIOP	529	92.6	44	8.3	0.32	0.24	0.51	0.08	0.66	0.10	0.79	0.00
POLDER3 L	9926	86.3	1050	10.6	0.43	0.14	0.33	0.00	0.67	0.07	0.62	−0.02
POLDER3 O	1393	56.8	99	7.1	0.48	0.12	0.31	0.02	0.6	0.07	0.57	−0.01
SeaWiFS L	5795	47.5	306	5.3	0.81	0.1	0.79	0.02	0.85	0.07	0.89	0.01
SeaWiFS O	3665	82.4	277	7.6	0.61	0.12	0.94	0.03	0.81	0.06	0.89	0.02

Table 3. (Continued).

Dataset	N_{filt}	N_{filt}/N_{tot} (%)	N_{out}	N_{filt}/N_{out} (%)	Complete data				Outliers removed			
					R^2	RMSE	Slope	Intercept	R^2	RMSE	Slope	Intercept
Winter												
TMODIS DT	6229	64.4	253	4.1	0.79	0.11	0.76	0.03	0.84	0.08	0.86	0.02
TMODIS DB	826	37.0	82	9.9	0.65	0.23	0.9	0.08	0.81	0.13	0.9	0.05
TMODIS O	3297	99.8	140	4.2	0.72	0.09	0.98	0.03	0.87	0.05	0.93	0.03
AMODIS DT	4945	58.6	238	4.8	0.78	0.13	0.77	0.03	0.83	0.09	0.88	0.02
AMODIS DB	3052	39.9	278	9.1	0.62	0.21	0.84	0.06	0.81	0.12	0.91	0.02
AMODIS O	3319	99.5	183	5.5	0.74	0.08	0.84	0.03	0.84	0.04	0.92	0.02
MISR	2701	99.9	179	6.6	0.75	0.11	0.54	0.06	0.82	0.05	0.77	0.04
OMI	8569	93.9	279	3.3	0.44	0.24	0.63	0.17	0.53	0.19	0.69	0.14
CALIOP	313	91.3	29	9.3	0.43	0.25	0.37	0.09	0.71	0.10	0.72	0.02
POLDER3 L	4954	87.1	488	9.9	0.35	0.21	0.15	0.02	0.56	0.08	0.4	0.00
POLDER3 O	792	57.4	45	5.7	0.54	0.11	0.39	0.01	0.59	0.08	0.54	−0.01
SeaWiFS L	3063	46.1	163	5.3	0.69	0.15	0.65	0.05	0.76	0.1	0.8	0.03
SeaWiFS O	1917	81.6	137	7.1	0.57	0.12	0.89	0.05	0.75	0.07	0.84	0.03
Spring												
TMODIS DT	12 990	74.0	505	3.9	0.79	0.11	0.92	0.03	0.85	0.08	0.96	0.01
TMODIS DB	746	34.4	33	4.4	0.65	0.3	0.78	0.12	0.69	0.21	0.84	0.07
TMODIS O	3464	99.7	130	3.8	0.85	0.09	1.05	0.03	0.88	0.06	0.97	0.04
AMODIS DT	11 266	70.7	511	4.5	0.78	0.12	0.96	0.03	0.84	0.08	0.97	0.02
AMODIS DB	3079	35.6	163	5.3	0.63	0.27	0.83	0.09	0.73	0.19	0.86	0.06
AMODIS O	3625	99.8	160	4.4	0.81	0.09	0.99	0.03	0.87	0.06	0.92	0.04
MISR	4016	99.9	260	6.5	0.76	0.13	0.64	0.08	0.86	0.06	0.86	0.04
OMI	12 170	96.5	446	3.7	0.45	0.29	0.77	0.18	0.55	0.22	0.79	0.15
CALIOP	439	93.2	41	9.3	0.37	0.25	0.56	0.05	0.71	0.12	0.81	−0.02
POLDER3 L	7809	87.9	1170	15	0.25	0.27	0.11	0.02	0.52	0.10	0.4	−0.01
POLDER3 O	1443	61.7	162	11.2	0.38	0.18	0.24	0.04	0.56	0.09	0.52	0.00
SeaWiFS L	4345	45.4	306	7.0	0.78	0.15	0.76	0.05	0.87	0.09	0.91	0.02
SeaWiFS O	3038	82.2	221	7.3	0.68	0.15	1.05	0.02	0.83	0.07	0.95	0.02
Summer												
TMODIS DT	21 998	75.6	519	2.4	0.76	0.1	1.01	0.00	0.78	0.08	0.98	0.00
TMODIS DB	1437	31.5	91	6.3	0.65	0.24	0.91	0.04	0.77	0.14	0.90	0.02
TMODIS O	5362	99.6	247	4.6	0.84	0.09	1.06	0.02	0.89	0.06	0.98	0.03
AMODIS DT	19 685	72.3	551	2.8	0.76	0.1	1.05	0.01	0.79	0.08	1.00	0.01
AMODIS DB	3486	30.1	228	6.5	0.62	0.24	0.90	0.06	0.74	0.15	0.91	0.04
AMODIS O	5711	99.5	276	4.8	0.84	0.08	1.00	0.02	0.88	0.05	0.95	0.02
MISR	5378	99.9	222	4.1	0.73	0.13	0.64	0.07	0.83	0.06	0.86	0.03
OMI	17 850	97.1	542	3.0	0.35	0.25	0.73	0.18	0.45	0.2	0.76	0.15
CALIOP	604	92.1	40	6.6	0.33	0.18	0.52	0.05	0.6	0.11	0.76	0.00
POLDER3 L	9185	84.9	1125	12.2	0.22	0.19	0.15	0.02	0.53	0.07	0.52	−0.01
POLDER3 O	1772	62.0	192	10.8	0.32	0.17	0.20	0.04	0.6	0.07	0.59	0.00
SeaWiFS L	5102	36.9	243	4.8	0.67	0.13	0.70	0.04	0.75	0.08	0.85	0.01
SeaWiFS O	4713	83.4	286	6.1	0.68	0.11	1.00	0.03	0.82	0.06	0.93	0.02

Title Page

Abstract | Introduction

Conclusions | References

Tables | Figures

|◄ | ►|

◄ | ►

Back | Close

Full Screen / Esc

Printer-friendly Version

Interactive Discussion

Coherent uncertainty analysis of aerosol measurements

M. Petrenko and
C. Ichoku

Table 4. Linear fit correlation coefficient (R^2) between the collocated spaceborne and ground-based observations of AOD estimated at the stations that coincide with different IGBP land cover types. Empty cells indicate no collocated data available from a specific sensor over a specific land cover type. No AERONET stations are available at the areas occupied by Deciduous needleleaf forest. The statistics were calculated based on the data that was pre-filtered by QA and screened of outliers as described in Sects. 4 and 5. A graphical representation of this table is in Fig. 13.

	TMODIS DT	TMODIS DB	TMODIS O	AMODIS DT	AMODIS DB	AMODIS O	MISR	OMI	CALIOP	POLDER3 L	POLDER3 O	SeaWiFS L	SeaWiFS O
Water			0.74			0.80	0.72	0.39	0.59			0.55	0.68
Evergreen needleleaf forest	0.78			0.79	0.71		0.74	0.33	0.59	0.55		0.66	
Evergreen broadleaf forest	0.85	1.00		0.85			0.89	0.53	0.17	0.70		0.94	
Deciduous broadleaf forest	0.84			0.87			0.84	0.55	0.27	0.70		0.84	
Mixed forests	0.78			0.82			0.70	0.42	0.61	0.65		0.69	
Closed shrubland	0.51	0.74		0.63	0.85		0.81	0.50	0.88	0.33		0.65	
Open shrublands	0.67	0.52		0.62	0.65		0.64	0.31	0.68	0.32		0.54	
Woody savannas	0.83	0.91		0.86	0.86		0.63	0.66	0.34	0.54		0.79	
Savannas	0.73	0.69		0.80	0.67		0.75	0.53	0.59	0.67		0.78	
Grasslands	0.56	0.73		0.67	0.43		0.70	0.48	0.40	0.44		0.55	
Permanent wetlands	0.74			0.76			0.77	0.31	0.54	0.39		0.02	
Croplands	0.78	0.72		0.78	0.62		0.80	0.47	0.56	0.49		0.68	
Urban and built-up	0.70	0.64		0.70	0.59		0.76	0.43	0.51	0.44		0.62	
Cropland/ natural veget. mosaic	0.77			0.79	0.49		0.83	0.54	0.46	0.56		0.72	
Snow and ice	0.26			0.27			0.83		0.03	0.53			
Barren or sparsely vegetated	0.60	0.57		0.62	0.34		0.78	0.29	0.58	0.33		0.36	

Title Page

Abstract | Introduction

Conclusions | References

Tables | Figures

|◀ | ▶|

◀ | ▶

Back | Close

Full Screen / Esc

Printer-friendly Version

Interactive Discussion

Table 5. Root mean square error (RMSE) between the collocated spaceborne and ground-based observations of AOD estimated at the stations that coincide with different IGBP land cover types. Empty cells indicate no collocated data available from a specific sensor over a specific land cover type. No AERONET stations are available at the areas occupied by Deciduous needleleaf forest. The statistics were calculated based on the data that was pre-filtered by QA and screened of outliers as described in Sects. 4 and 5. A graphical representation of this table is in Fig. 14.

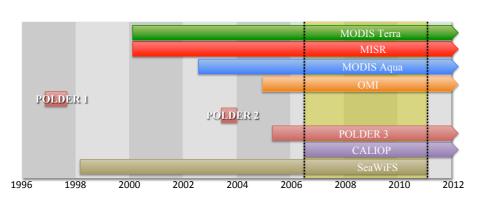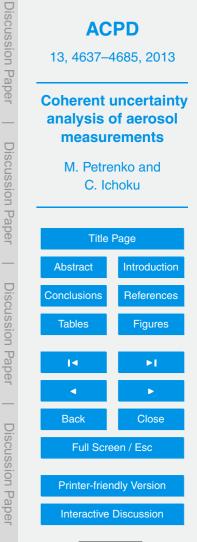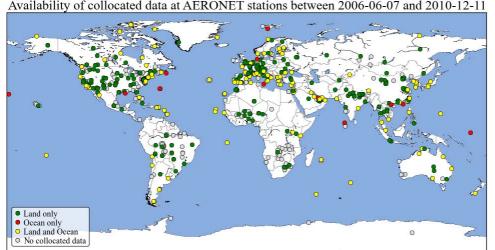|	TMODIS DT	TMODIS DB	TMODIS O	AMODIS DT	AMODIS DB	AMODIS O	MISR	OMI	CALIOP	POLDER3 L	POLDER3 O	SeaWiFS L	SeaWiFS O
Water			0.06			0.05	0.07	0.17	0.12		0.08		0.09
Evergreen needleleaf forest	0.07	0.09		0.06	0.30		0.06	0.18	0.08	0.06		0.05	
Evergreen broadleaf forest	0.10	0.80		0.09	0.30		0.11	0.25	0.35	0.07		0.23	
Deciduous broadleaf forest	0.06			0.06			0.04	0.12	0.11	0.05		0.05	
Mixed forests	0.08			0.07			0.04	0.14	0.12	0.06		0.05	
Closed shrubland	0.09	0.05		0.08	0.05		0.06	0.18	0.04	0.09		0.06	
Open shrublands	0.10	0.10		0.09	0.14		0.08	0.23	0.11	0.13		0.08	
Woody savannas	0.08	0.27		0.09	0.23		0.09	0.24	0.18	0.15		0.08	
Savannas	0.11	0.17		0.10	0.17		0.08	0.27	0.12	0.12		0.14	
Grasslands	0.10	0.18		0.09	0.15		0.05	0.20	0.12	0.10		0.08	
Permanent wetlands	0.07			0.06			0.06	0.17	0.11	0.09		0.13	
Croplands	0.08	0.16		0.09	0.22		0.08	0.19	0.16	0.11		0.09	
Urban and built-up	0.09	0.13		0.09	0.16		0.07	0.21	0.13	0.10		0.10	
Cropland/natural veget. mosaic	0.07			0.08	0.19		0.10	0.14	0.20	0.09		0.11	
Snow and ice	0.11			0.14			0.02		0.10	0.02			
Barren or sparsely vegetated	0.11	0.16		0.12	0.11		0.06	0.39	0.11	0.12		0.11	

Discussion Paper | Discussion Paper | Discussion Paper | Discussion Paper | Discussion Paper

Title Page

Abstract | Introduction

Conclusions | References

Tables | Figures

◀ | ▶

◀ | ▶

Back | Close

Full Screen / Esc

Printer-friendly Version

Interactive Discussion

M. Petrenko and
C. Ichoku

Fig. 1. Periods of operation of major past and current aerosol-measuring satellite sensors. The pair of dotted vertical lines marks the "golden" period (between the start of CALIOP in July 2006 and the end of SeaWiFS in December 2010) when as many as seven of these sensors were measuring aerosols concurrently. The golden period was used as the base for the studies reported in the rest of this paper.
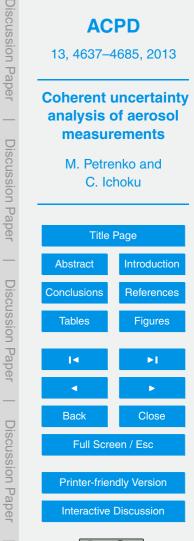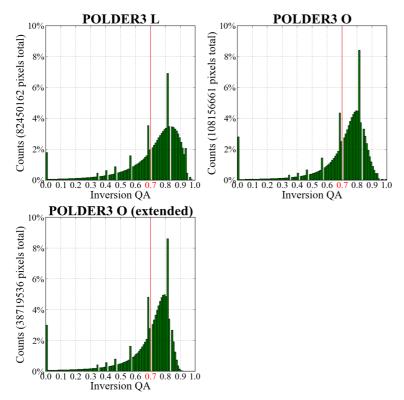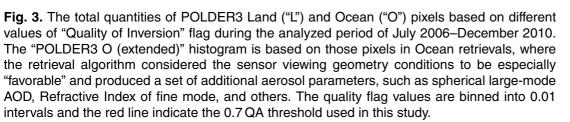
Availability of collocated data at AERONET stations between 2006-06-07 and 2010-12-11

Fig. 2. Distribution of AERONET stations used in the study. Green, red, and yellow colors indicate stations that can be classified as land only (226 sites), ocean only (12 sites), or both land and ocean (142 sites), respectively. The classification was established based on data availability in separate over-land and over-ocean datasets in MODIS, SeaWiFS, and POLDER aerosol products. Gray color indicates stations that do not have any collocated data for the studied period of time.

Fig. 3. The total quantities of POLDER3 Land ("L") and Ocean ("O") pixels based on different values of "Quality of Inversion" flag during the analyzed period of July 2006–December 2010. The "POLDER3 O (extended)" histogram is based on those pixels in Ocean retrievals, where the retrieval algorithm considered the sensor viewing geometry conditions to be especially "favorable" and produced a set of additional aerosol parameters, such as spherical large-mode AOD, Refractive Index of fine mode, and others. The quality flag values are binned into 0.01 intervals and the red line indicate the 0.7 QA threshold used in this study.

Discussion Paper | Discussion Paper | Discussion Paper | Discussion Paper |

Fig. 4. Effects of two different data QA filtering schemes on the accuracy of the global collocated spaceborne AOD, as discussed in Sect. 4. AERONET AOD data are shown on the X-axes, while AOD measured by spaceborne sensors are on the Y-axes. Color of each data point indicates the percentage of all data points that fall within 0.05 AOD of this point (in Cartesian coordinates). Left column displays the original unfiltered data with all QA values. Middle column displays the data *pre-filtered* by QA, where individual pixels in each data sample were filtered based on their QA values *before* calculating the mean value of the sample. Right column shows the data *post-filtered* by QA, where the mean of each sample was calculated based on all pixels in the sample; *after* this, the whole sample was rejected if at least half of the pixels in the sample had QA values below the specified threshold. Note that OMI data have better properties when pre-filtered, while Terra MODIS – Deep Blue data are in a better agreement with AERONET AOD when pos-filtered.

Fig. 5. Impact of QA screening on the statistical properties of AOD retrieved by different sensors over Djougou, Benin. The top part of the figure shows scatter plots of 2 yr of data that is unfiltered (left) or pre-filtered (right) by QA. It can be observed that while filtering improved the properties of certain datasets, it degraded the properties of the others, particularly Aqua MODIS Deep Blue and OMI. This effect can be partially explained by observing that the retrieval algorithms can mistakenly assign bad QA to pixels with good retrievals, as demonstrated in a high-AOD event in the bottom part of the picture, e.g. see AMODIS DB on 11 and 19 December.

Fig. 6. Regression fits of AERONET AOD (x-axes) to AOD measured by spaceborne sensors (y-axes). Satellite data were pre-screened by QA as explained in Sect. 4. The color of each data point indicates the percentage of all data points on the plot that fall within 0.05 AOD of this point (in Cartesian coordinates). Scatter plot in the green frame demonstrates the results of the possible data outlier detection and removal procedure described in Sect. 5.
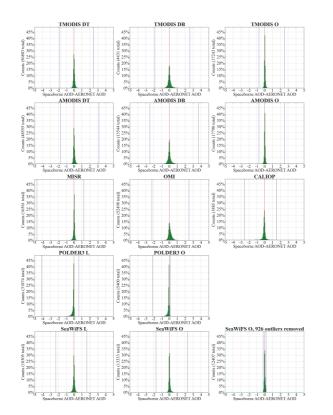
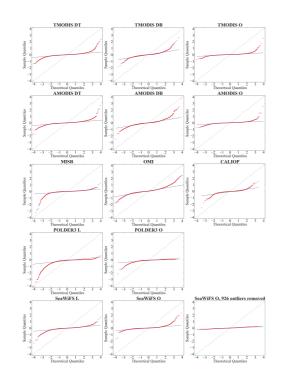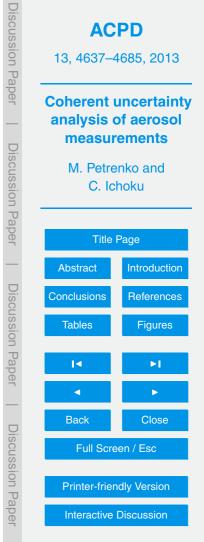**Fig. 7.** Distribution of the difference (residuals) between Spaceborne AOD and AERONET AOD. Satellite data were pre-screened by QA as explained in Sect. 4. In each histogram, the data are split into equal-length bins of 0.05 AOD. The red vertical line indicates the residual of 0 AOD, while the blue lines mark minimum and maximum residuals of each distribution. Histogram in the green frame demonstrates the results of the possible data outlier detection and removal procedure described in Sect. 5.

Title Page

Abstract | Introduction

Conclusions | References

Tables | Figures

|◄ | ►|

◄ | ►

Back | Close

Full Screen / Esc

Fig. 8. Normality of the difference between Spaceborne AOD and AERONET AOD. In each plot, points closely following the blue fitted line indicate the data that are approximately normally distributed. Curvatures around the center of the straight line represent the departure from the normality and indicate a presence of possible outliers, particularly at the tails of the distributions. The difference in the slope and offset of the fitted blue line from the gray 1:1 line indicates a deviation from the standard location (i.e. mean = 0) and scale (i.e. standard deviation = 1) of the normal distribution. Satellite data were pre-screened by QA as explained in Sect. 4. Plot in the green frame demonstrates the results of the possible data outlier detection and removal procedure described in Sect. 5.
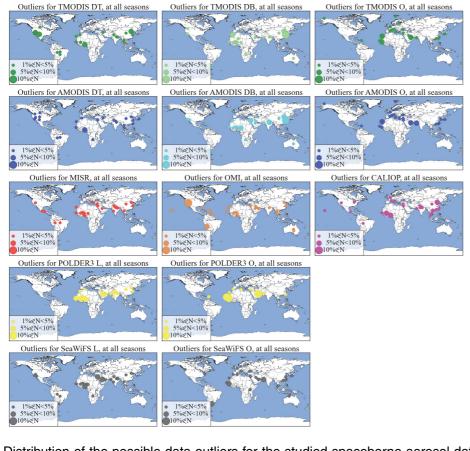
Title Page

Abstract | Introduction

Conclusions | References

Tables | Figures

◄ | ►

◄ | ►

Back | Close

Full Screen / Esc

Printer-friendly Version

Interactive Discussion

Fig. 9. Distribution of the possible data outliers for the studied spaceborne aerosol data sets. Displayed values are percentages from all outliers detected for each of the data sets as listed in the 4th column of Table 3. Stations with less than 1 % from the total number of outliers are not shown. The statistical technique for detection and removal of the possible data outliers is described in Sect. 5.
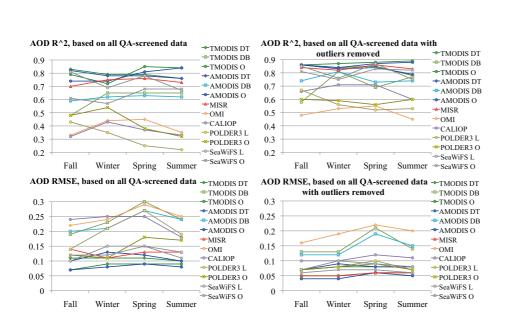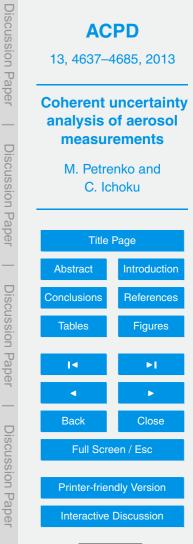
Title Page

Abstract | Introduction

Conclusions | References

Tables | Figures

◄ | ►

◄ | ►

Back | Close

Full Screen / Esc

Printer-friendly Version

Interactive Discussion

Fig. 10. Seasonal dependence of squared linear fit correlation coefficient (R^2) and root mean square error (RMSE) statistics between the collocated spaceborne and ground-based (AERONET) observations of AOD, based on the data in Table 3.
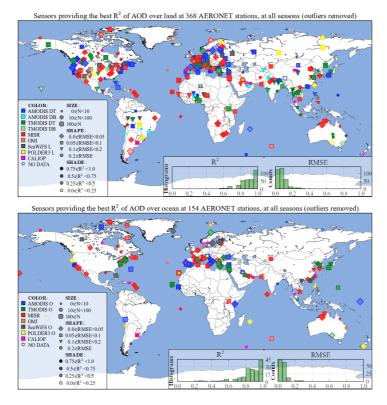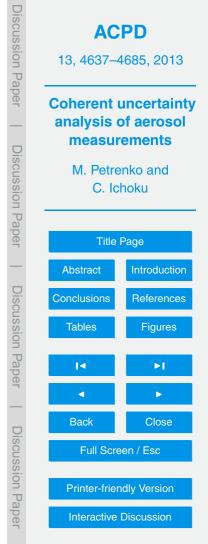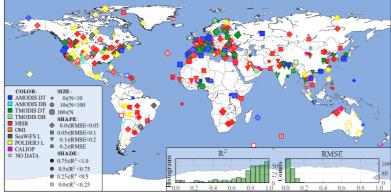
Fig. 11. Spaceborne datasets with the best correlation (R^2) of the retrieved AOD to the AOD measured by inland (top) and coastal or island-based (bottom) AERONET sites. The intensity of marker shading indicates the degree of correlation. Marker shape indicates the range of root mean square error (RMSE) associated with the displayed best R^2. Finally, marker size corresponds to the number of collocated data points used to compute the displayed statistics. Histograms in the bottom insets highlight the distribution of these statistics over all sites based on bins of 0.05 AOD. The statistics were calculated based on the data that were pre-filtered by QA and screened of outliers as described in Sects. 4 and 5.
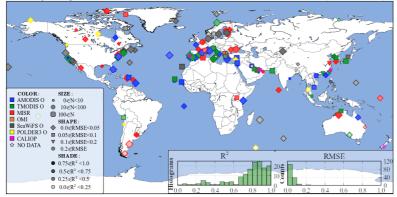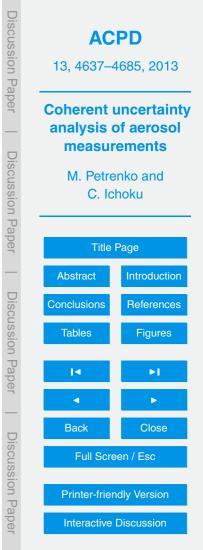
Fig. 12. Spaceborne datasets with the best root mean square error (RMSE) of the retrieved AOD to the AOD measured by inland (top) and coastal or island-based (bottom) AERONET sites. The symbols used are the same as the symbols in Fig. 11. The statistics were calculated based on the data that were pre-filtered by QA and screened of outliers as described in Sects. 4 and 5.
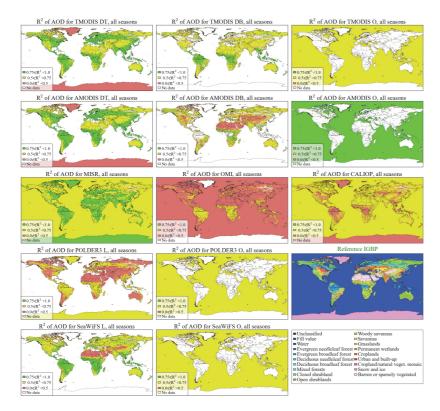
Fig. 13. Land cover type dependence of squared linear fit correlation coefficient (R^2) between the collocated spaceborne and ground-based (AERONET) observations of AOD. Areas corresponding to each IGBP land cover type (bottom right inset) are colored based on the average of the data from those AERONET sites that reside in these areas. The statistics were calculated based on data that were pre-filtered by QA and screened of outliers as described in Sects. 4 and 5.

Title Page

Abstract | Introduction

Conclusions | References

Tables | Figures

◀ | ▶

◀ | ▶

Back | Close

Full Screen / Esc

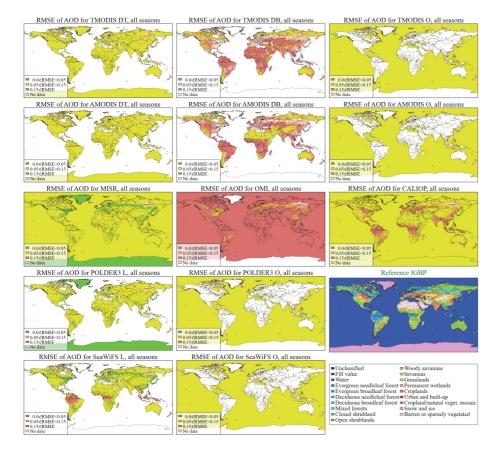Printer-friendly Version

Interactive Discussion

Fig. 14. Land cover type dependence of root mean square error (RMSE) between the collocated spaceborne and ground-based (AERONET) observations of AOD. Areas corresponding to each IGBP land cover type (bottom right inset) are colored based on the average of the data from those AERONET sites that reside in these areas. The statistics were calculated based on the data that were pre-filtered by QA and screened of outliers as described in Sects. 4 and 5.

Coherent uncertainty analysis of aerosol measurements

M. Petrenko and
C. Ichoku

Title Page

Abstract | Introduction

Conclusions | References

Tables | Figures

◀◀ | ▶▶

◀ | ▶

Back | Close

Full Screen / Esc

Printer-friendly Version

Interactive Discussion